JMolMed

ORIGINAL ARTICLE

Chemically modified curcumin (CMC2.24) alleviates osteoarthritis progression by restoring cartilage homeostasis and inhibiting chondrocyte apoptosis via the NF-κB/HIF-2α axis

Yan Zhou[1] · Jianghua Ming[1] · Ming Deng[1] · Yaming Li[1] · Bochun Li[2] · Jia Li[3] · Yonggang Ma[1] · Zhonghui Chen[1] · Guirong Wang[4] · Shiqing Liu[1]

Abstract

The disorders of cartilage homeostasis and chondrocyte apoptosis are major events in the pathogenesis of osteoarthritis (OA). Herein, we aim to assess the chondroprotective effect and underlying mechanisms of a novel chemically modified curcumin, CMC2.24, in modulating extracellular matrix (ECM) homeostasis and inhibiting chondrocyte apoptosis. Rats underwent the anterior cruciate ligament transection, and medial menisci resection was treated by intra-articular injection with CMC2.24. In an in vitro study, rat chondrocytes were pretreated with CMC2.24 before stimulation with sodium nitroprusside (SNP). Results from in vivo studies demonstrated that the intra-articular administration of CMC2.24 ameliorated osteoarthritic cartilage destruction by promoting collagen 2a1 production and inhibited cartilage degradation and apoptosis by suppressing hypoxia-inducible factor-2a (Hif-2α), matrix metalloproteinase-3, runt-related transcription factor 2, cleaved caspase-3, and vascular endothelial growth factor and the phosphorylation of IκBα and NF-κB p65. The in vitro results revealed that CMC2.24 exhibited a strong inhibitory effect on SNP-induced chondrocyte catabolism and apoptosis. The SNP-enhanced expression of Hif-2α, a catabolic and apoptotic factor, decreased in a dose-dependent manner after CMC2.24 treatment. CMC2.24 pretreatment effectively inhibited SNP-induced IκBα and NF-κB p65 phosphorylation in rat chondrocytes, whereas pretreatment with the NF-κB antagonist BMS-345541 significantly enhanced the effects of CMC2.24. Overall, these results demonstrated that CMC2.24 attenuates OA progression by modulating ECM homeostasis and chondrocyte apoptosis by suppressing the NF-κB/Hif-2α axis, thus providing a new perspective for therapeutic strategies in OA.

Key messages

- Intra-articular injection of CMC2.24 ameliorated osteoarthritic cartilage destruction.
- CMC2.24 promoted cell viability and decreased SNP-induced apoptotic gene expression.
- SNP-induced activation of Hif-2α is inhibited by CMC2.24.
- CMC2.24 inhibits NF-κB/Hif-2α axis activation to modulate ECM homeostasis and inhibit chondrocyte apoptosis.

Keywords Osteoarthritis · Chemically modified curcumin (CMC2.24) · Cartilage homeostasis · NF-κB · Hif-2α

✉ Guirong Wang
  Wangg@upstate.edu

✉ Shiqing Liu
  liusqrm@163.com

1 Department of Orthopedics, Central Laboratory, Renmin Hospital of Wuhan University, Wuhan 430060, China

2 Department of Rehabilitation, Wuhan Union Hospital, Huazhong University of Science and Technology, Wuhan 430022, China

3 College of Acupuncture and Bone Injury, Hubei University of Chinese Medicine, Wuhan 430061, China

4 Department of Surgery, SUNY Upstate Medical University, 750 E. Adams St., Syracuse, NY 13210, USA

Introduction

Increased inflammatory component, mechanical overload, metabolic alterations, and cell senescence result in the deterioration of the articular cartilage in the knee joint, thus leading to osteoarthritis (OA), a widespread and age-related joint disorder [1, 2]. OA, characterized by an initial loss of proteoglycan in cartilage, subchondral bone modification, and osteophyte formation in the joint edge, is a challenging disease because effective disease-specific drugs are currently unavailable [3]. OA is an active dynamic change caused by the imbalance between joint tissue repair and destruction, rather than

🙂 Springer

a commonly described passive degenerative disease or the so-called wear-and-tear disease [4]. In a degenerative cartilage, the degradation of extracellular matrix (ECM) is caused by the stimulation of catabolic factors, such as matrix metalloproteinases (MMPs) and aggrecanases in chondrocytes [5, 6]. Hypertrophic chondrocytes display enhanced synthetic activity when repairing themselves, but this activity leads to the production of matrix degradation products and pro-inflammatory mediators, thereby disrupting chondrocyte function and stimulating adjacent synovial cell proliferation and pro-inflammatory responses [7]. Cell death with the morphological and molecular characteristics of apoptosis has been detected in OA cartilage, suggesting that chondrocyte death/survival plays a key role in the pathogenesis of OA [8]. Thus, the identification of chondrocyte apoptosis biomarkers can promote the development of novel therapies for eliminating the cause or at least slowing down the process of OA degradation [9]. Therefore, maintaining the optimal equilibrium of anabolic-catabolic signaling and inhibition of chondrocyte apoptosis are potential strategies in OA.

Since the development of surgically induced rat OA models, several molecules and relevant signaling pathways involved in its pathophysiological processes have been identified. Wherein, hypoxia-inducible factor-2a (Hif-2α), which plays an important role in the development of OA, is the transcriptional factor of representative cartilage-degrading enzymes, such as MMP-3 [10, 11]. The activation of the nuclear factor kappa-B (NF-κB) signaling pathway is closely related to the development of OA and other factors of the downstream of Hif-2α [12, 13]. Continuous NF-κB activation stimulates regulatory transcription factors, such as Hif-2α and runt-related transcription factor 2 (RUNX2), which enhance the production of disintegrin and metalloproteinase with thrombospondin motifs-5 enzymes and MMP-13, thereby promoting the transformation of chondrocytes from a pre-hypertrophic state to a terminal hypertrophic state [14]. Previous studies have shown that OA is aggravated by increase in chondrocyte apoptosis owing to the homozygous knockout of Rela, the main subunit of the NF-κB pathway, in adult chondrocytes, whereas OA is suppressed by the down-regulation of Hif-2α and MMP-3 through heterozygous knockout [15, 16]. Rela is indispensable to chondrocyte survival through the transcriptional induction of anti-apoptotic genes, and the activation of NF-κB signaling results in the induction of Hif-2α and catabolic factors in mouse primary chondrocytes [17]. Therefore, NF-κB signaling is critical for articular cartilage homeostasis and chondrocyte apoptosis in the prevention and treatment of OA.

In the development of novel therapeutic agents, an appropriate and common strategy is to optimize of the pharmacological properties and improve the efficacy of drugs through chemical modification [18–20]. Curcumin, a component of turmeric, is usually extracted from the rhizomes of *Curcuma longa*, which possesses several pharmacological properties, including anti-inflammatory and antioxidant effects, and has been broadly used in traditional Chinese medicine for ameliorating OA [21, 22]. Curcumin selectively inhibits the activities of inducible MMPs and down-regulates the expression of pro-inflammatory cytokines through the modulation of NF-κB and related signaling pathways [23]. A novel chemically modified curcumin, CMC2.24 (structure shown in Fig. 1b), is more efficient than natural curcumins in inhibiting apoptosis, inflammation, and inducible MMPs, all of which lead to tissue injury [24]. The pharmacokinetic properties of curcumin were upgraded by adding an electron-withdrawing group, which increased the acidity of the enolic system. This compound, CMC2.24, phenylamino carbonyl curcumin, is triketonic (enhancing its zinc-binding characteristics) with diketonic active site on tetracycline and traditional/natural curcumin compounds, which are effective in cell and organ culture, chronic inflammation, and other animal models of disease [25, 26]. CMC2.24 showed significantly enhanced bioactivity, and bio-availability, and solubility with decreased toxicity [27]. The oral administration of CMC2.24 reduced inflammatory cytokines and modulated MMP level in a rabbit OA model [28]. Nevertheless, data about therapeutic mechanisms for CMC2.24 on ECM homeostasis and chondrocyte apoptosis are unavailable. In the present study, we performed intra-articular injections of CMC2.24 into the knee joints of rats with OA induced by surgical treatment and then histologically analyzed the development of OA and changes in the expression of OA-related proteins. We further examined the inhibitory effects of CMC2.24 on sodium nitroprusside (SNP)-induced apoptosis in rat chondrocytes and elucidated the underlying mechanisms of the NF-κB/Hif-2α axis involvement.

Material and methods

Chemicals and reagents

CMC2.24 compound with 99.5% purity [20] was kindly provided by Dr. Francis Johnson (Chem-Master Intl. Inc., Hauppauge, NY, USA). CMC2.24 was completely dissolved in dimethyl sulfoxide (DMSO) to a final concentration of 0.05%. Medium plus 0.05% DMSO was used as a solvent control. Glyceraldehyde-3-phosphate dehydrogenase (GAPDH) (Cat# ab37168), MMP-3 (Cat# ab52915), RUNX2 (Cat# ab23981), collagen 2a1 (Col2a1) (Cat# ab34712), Bcl-2 (Cat# ab196495), and vascular endothelial growth factor (VEGF) (Cat# ab214424) antibodies were obtained from Abcam (Cambridge, UK). Hif-2α (Cat# NB100-122) was obtained from Novus Biologicals (Littleton, Colorado, USA). Cleaved caspase-3 (Cat# 9664), phosphorylated-p65 (p-p65) (Cat# 3033), p65 (Cat# 8242), p-IκBα (Cat# 2859), and IκBα (Cat# 9242) antibodies were
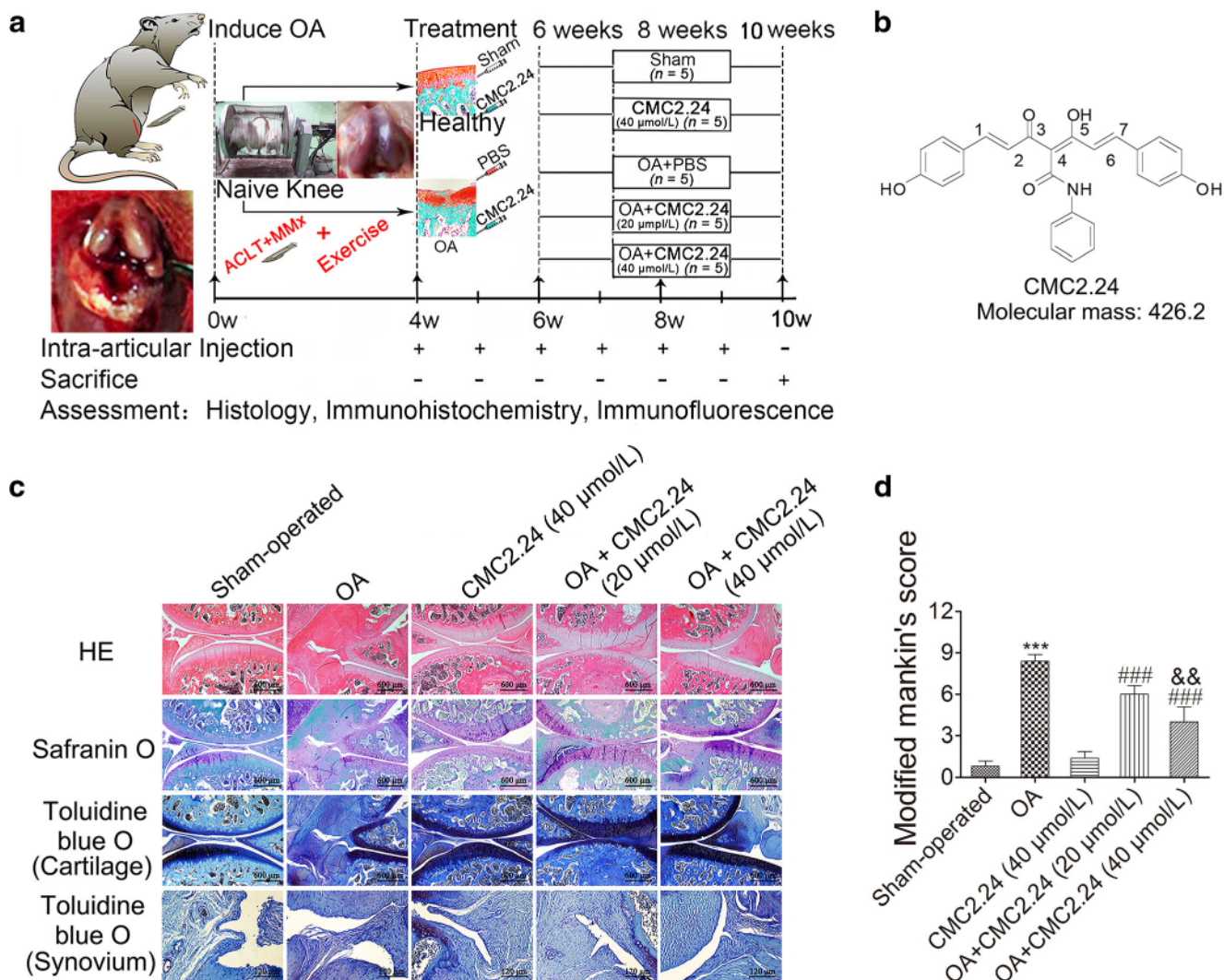
Fig. 1 An overview of study timelines and the rescue of cartilage degeneration by CMC2.24 in OA model rats. **a** ACLT + MMx rats were put into an electronic rotator cage for 30 min per day as a means of inducing OA model beginning 1 week post-surgery. At 4 weeks post-surgery, animals were injected intra-articularly with different concentrations of CMC2.24. PBS was used as controls in sham and OA-model animals. **b** The structure of CMC2.24. **c** H&E, Safranin O, and toluidine blue O-stained tissue histology in rat articular cartilage at 10 weeks post-surgery. **d** The modified Mankin scores were assigned to tissue samples. Data were expressed as mean ± SEM ($n = 5$). $^{***}P < 0.001$ vs. the sham-operated group; $^{###}P < 0.001$ vs. the OA-induction group; $^{\&}P < 0.05$ vs. OA + CMC2.24 (20 μM) group

ordered from Cell Signaling Technology (Danvers, MA, USA). BMS-345541 (Cat# HY-10518) was obtained from MedChem Express (Monmouth Junction, NJ, USA). SNP (Cat# 1008) was procured from Youcare Pharmaceutical Group Co., Ltd. (Beijing, China).

Rat OA model and CMC2.24 treatment experiments

Male Sprague–Dawley (SD) rats (body weight: 200–250 g) were purchased from the Center for Animal Experiment/ABSL-III Laboratory, Wuhan University. Animals were maintained under standard conditions (12-h light/12-h dark cycle at 20–24 °C and 50–55% humidity) for 1 week and then randomized into five groups (five rats/group), namely, the sham-operated, CMC2.24 (high-dose), OA-induced, OA + CMC2.24 (low-dose), and OA + CMC2.24 (high-dose) groups (Fig. 1a). The animals were anesthetized intraperitoneally with trichloroacetaldehyde hydrate (300 mg/kg) in sterile saline. The OA model was induced through anterior cruciate ligament transection and medial menisci resection (ACLT + MMx) as previously described [29]. The rats were injected with antibiotics (1.0–1.3 mg/cefotiam hydrochloride) intramuscularly for 3 days after surgery. In the first week after surgery, the rats were transferred to an electric rotating cage. The cage was 20 cm in diameter and 22 cm in transverse diameter, with constantly rotating activity (speed 15 rpm) for 30 min per day. Four weeks after operation, the right knee joint of the rats in the low- and high-dose CMC2.24 treatment

groups were injected with 30 μl of 20 and 40 μM CMC2.24, respectively, weekly. The rats in the sham and OA-induction groups received intra-articular injection of 30 μl phosphate-buffered saline (PBS). Intra-articular injections were performed once a week at fixed time points for a total of six injections. The animals were sacrificed 10 weeks post-operation through cardiac exsanguination. The Animal Care and Use Committee of Medical School, Wuhan University, approved all the animal studies (WDRM 20160104).

Evaluation of cartilage destruction and immunohistochemistry

After dissection, the right knee joints were isolated and fixed for 24 h with 4% paraformaldehyde, then decalcified for 4 weeks with Calci-Clear slow solution (10% (w/v) ethylene diamine tetraacetic acid, pH 7.4) before they were embedded in paraffin wax. Joint tissues cut into serial 5 μm sagittal sections were stained with hematoxylin and eosin (H&E), toluidine blue-O, and Safranin-O. Then, two blinded observers conducted a semiquantitative scoring of cartilage histopathology according to a modified Mankin scoring system [30]. MMP-3, RUNX2, Col2a1, cleaved caspase-3, VEGF, p-p65, and p-IκB-α protein expression levels in the joint cartilages were analyzed through immunohistochemistry. Hif-2α expression in articular cartilage was assessed through immunofluorescence. After Hif-2α (1:200 dilution) antibody staining overnight at 4 °C, a fluorescent secondary antibody labeled with CY3 (Boster Biological Engineering, Wuhan, China) was visualized for 1 h, followed by fluorescence microscope (Olympus Corporation, Tokyo, Japan). Immunoreactive integrated mean densities in the sections were measured using Image-Pro Plus 6.0 (Media Cybernetics Co., USA).

TUNEL assay

DNA fragmentation in cartilage chondrocytes undergoing programmed cell death was conducted according to the instructions in the in situ cell death detection kit (KeyGEN Biotech, Nanjing, China) used. Briefly, the cartilage sagittal sections of the knee joints were pretreated for 15 min with 20 μg/ml proteinase K (Dako, Glostrup, Denmark); then apoptotic chondrocytes in the articular cartilages were labeled. Apoptotic cells in tissues from each group were counted using five random high-power fields (× 100).

Rat chondrocyte culture and treatment

Primary articular chondrocytes were isolated from the joint articular cartilages of 5-day-old SD rats. Minced tissues were digested at 37 °C for 4–5 h with 0.2% type II collagenase. Suspended chondrocytes were cultured in a monolayer and suspended in complete Dulbecco's modified Eagle's medium complemented with 10% fetal bovine serum (Gibco-BRL, Maryland, USA) and penicillin/streptomycin. The third passage chondrocytes were replated in a complete growth media for 24 h and treated with a range of CMC2.24 concentrations (5 and 10 μM) in the presence or absence of BMS-345541 (5 μM) for 2 h. Then, 0.75 mM SNP co-treatment was performed for 24 h. The cells were seeded at a density of approximately 1.2 to 1.5 * 10^6/well in a six-well plate. All the protocols were approved by the Institutional Ethics Committee of Medical School, Wuhan University.

Cell viability

Cell viability was examined according to the provided protocols of the cell counting kit-8 (CCK-8) assay kit (Dojindo Laboratories, Kumamoto, Japan). Briefly, chondrocytes were cultured in 96-well culture plates for 24 h at 5000 cells per well prior to treatments; then a range of CMC2.24 concentrations were added to cells for 12, 24, and 48 h. The cells were incubated at 37 °C for 1–4 h using 10% CCK-8 reagents. Optical density (OD) 450 nm values were detected with an ELISA reader (Bio-Tek, Model EXL800, USA).

Evaluation of apoptosis

Quantification of apoptotic cells were assessed using flow cytometry (FCM) according to the provided protocols of Annexin V fluorescein isothiocyanate (FITC)/propidium iodide (PI) apoptosis kit (MultiSciences Biotech Co., Ltd., Hangzhou, China). Briefly, cells and cultural supernatants were harvested using 0.25% trypsin and resuspended in 500 μl of binding buffer, and 5 μl of PI and 5 μl of FITC-annexin V were used in incubating the cells for 15–20 min. The percentage of total apoptotic cells was determined using a flow cytometer (Becton Dickinson, USA).

Immunofluorescence assay

For the immunofluorescence assay, adherent chondrocytes with 70% confluency were grown on coverslips and treated after starvation for 12 h. The cells were fixed for 20 min with 4% paraformaldehyde at 37 °C, then permeabilized and blocked at 4 °C for 10 min with 0.1% Triton X-100 solution (Beyotime, Jiangsu, China) and 1% bovine serum albumin. Primary antibodies against NF-κB p65 (1:400 dilution) were used in probing the samples at 4 °C for 2 h. The cells were then washed again and incubated with a FITC-conjugated secondary antibody (Boster Biological Engineering, Wuhan, China) for 1 h, and DAPI was used for unclear staining, and an Olympus microscope (Olympus Corporation, Tokyo, Japan) was used in imaging the cells.

Western blotting

The extracted cellular proteins were resolved using sodium dodecyl sulfate-polyacrylamide gel electrophoresis, electrophoretically transferred to polyvinylidene difluoride (PVDF) membranes, and blocked at 37 °C with 5% (w/v) skim milk. The PVDF membranes were probed with primary antibodies against MMP-3 (1:2000 dilution), RUNX2 (1:1000 dilution), Col2a1 (1:500 dilution), cleaved caspase-3 (1:1000 dilution), Bcl-2 (1:1000 dilution), Hif-2α (1:500 dilution), VEGF (1:2000 dilution), NF-κB p65 (1:3000 dilution), p-p65 (1:500 dilution), IκB-α (1:2000 dilution), p-IκB-α (1:1000 dilution), and GAPDH (1:1000 dilution) at 4 °C overnight. Subsequently, the PVDF membranes were incubated at 4 °C for 1 h with HRP-conjugated secondary antibodies, and an enhanced chemiluminescence detection reagent (Amersham Biosciences, NJ, USA) was used in detecting proteins on an Odyssey infrared imaging system (LI-COR, NE, USA). Relative protein levels between groups were assessed after normalization to GAPDH.

Molecular docking

The X-ray crystal structures of IκB/NF-κB p65 homodimer complex (PDB code: 1OY3, re-solution: 2.05 Å) were downloaded from the RCSB Protein Data Bank (http://www.rcsb.org/). The chemical structure of CMC2.24 was drawn in accordance with the Tripos force field and Gasteiger-Huckel charge in the Sybyl package. CMC2.24 docking to the crystal structure of IκB/NF-κB p65 was simulated using the Surflex–Dock program in the Sybyl package. The images of 3D views were finally generated using UCSF PyMoL.

Statistical analysis

Data are analyzed using GraphPad Prism software (Version 6.0, San Diego, CA, USA). All values are given as mean ± standard error of the mean (SEM). Significant differences among groups were estimated using one-way ANOVA followed by Tukey's test (more than two groups) or a Student's t test (two groups) when the F statistic was significant. $P < 0.05$ was considered statistically significant.

Results

CMC2.24 inhibited the OA progression in rat OA model

Histological analysis was performed on the cartilage surfaces and matrix layers in the sections stained with H&E, Safranin O, and toluidine blue-O. As shown in Fig. 1c, compared with the sham-operated group, the OA-induction group showed irregular morphological structures in the articular cartilages and lower intensities of Safranin O staining, and CMC2.24-treated group exhibited less severe cartilage degradation, as evidenced by the increased thickness of articular cartilages and surface regularity. The modified Mankin scoring system was used in quantitatively evaluating cartilage degeneration after ACLT + MMx surgery (Fig. 1d). Compared with the OA-induction group, the intra-articular injection of CMC2.24 (20 and 40 μM) provided a high degree of protection against cartilage degeneration, as evidenced by considerable low Mankin scores. Histopathological changes in the synovia demonstrated marked synovial thickening in the OA-induction group, whereas a lower degree of synovial thickening was observed in the OA + CMC2.24 (20 and 40 μM) groups, demonstrating that CMC2.24 alleviated synovial inflammation.

CMC2.24 suppressed articular cartilage chondrocyte apoptosis in rat ACLT + MMx model

The biological effects of CMC2.24 on chondrocyte apoptosis were examined by TUNEL staining. As shown in Fig. 2a, compared with the sham-operated group, the OA-induction group had ubiquitous and strongly expressed TUNEL-positive cells in the articular cartilage zone. The number of TUNEL-positive cells in the CMC2.24-treated group considerably decreased in a dose-dependent manner. The percentage of apoptosis is shown in Fig. 2b, and statistically significant difference between the OA-induction group and the OA + CMC2.24 (20 and 40 μM) groups was observed.

CMC2.24 modulated ECM homeostasis and chondrocyte apoptosis by suppressing the activation of the NF-κB/Hif-2α axis

To investigate the mechanisms of cartilage protection in the CMC2.24-treated rats with ACLT + MMx surgery, pathological alterations in articular cartilage were examined through immunohistochemistry. As shown in Fig. 3, immunohistochemical analyses showed that in the OA-induction group, the immunoreactivities of MMP-3, cleaved caspase-3, VEGF, and RUNX2 expression in the articular cartilage zone were markedly higher than those in the sham-operated group, and these trends were reversed by the intra-articular injection of CMC2.24 from 20 to 40 μM. Moreover, immunohistochemistry suggested that Col2a1 synthesis in the growth plate and articular cartilage was significantly enhanced in the CMC2.24-treated group in a dosage-dependent manner compared with that in the OA-induction group.

The expression of Hif-2α (Fig. 4a) and the inhibition of the NF-κB signaling pathway (Fig. 4b) in the articular cartilage were explored through immunohistochemistry and
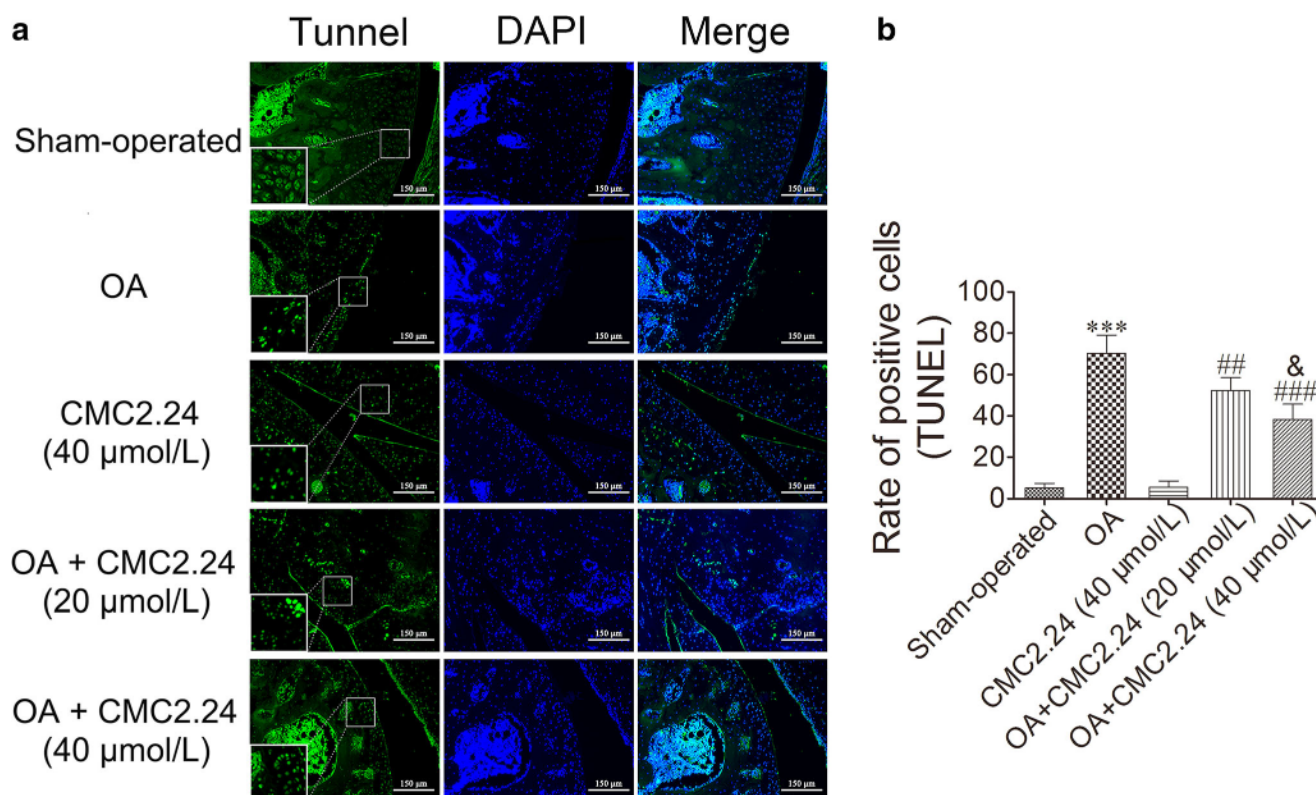
Fig. 2 Chondrocyte apoptosis was inhibited by CMC2.24 in vivo. CMC2.24 in different concentrations was injected into the right knee joint beginning 4 week post-surgery. At 10 weeks post-surgery, animals were sacrificed and the knee joints were collected for TUNEL analysis. **a** Representative TUNEL-stained section was used to assess apoptosis. **b** Apoptotic rates were calculated in TUNEL images. Data were expressed as mean ± SEM ($n = 5$). ***$P < 0.001$ vs. sham-operated group; ##$P < 0.01$ and ###$P < 0.001$ vs. OA induction group; &$P < 0.05$ vs. OA + CMC2.24 (20 μM) group

immunofluorescence. As shown in Fig. 4c, d, and e, the percentages of Hif-2α, p-p65, and p-IκB-α-positive cells were significantly higher in the OA-induced group than in the sham-operated group, and the expression levels of Hif-2α, p-p65, and p-IκB-α significantly decreased after the 20–40 μM CMC2.24 treatment.

CMC2.24 promoted cell viability and reduced SNP-induced chondrocyte apoptosis

The viability effect of CMC2.24 on chondrocytes was assessed through CCK-8 assay for 12, 24, and 48 h (Fig. 5a). Treatments with 20 and 30 μM CMC2.24 significantly reduced cell viability at 12, 24, and 48 h, and CMC2.24 at concentrations of up to 10 μM showed no observable cytotoxicity. Therefore, CMC2.24 concentrations from 1 to 10 μM were used in subsequent cell experiments. Whether CMC2.24 protects chondrocytes from SNP-induced apoptosis was determined through FCM, and Annexin V FITC/PI apoptosis kit was used. As shown in Fig. 5b, the ratio of total apoptotic cells in the 0.75 mM SNP-stimulated group was 50.1% ± 4.4%. The ratio was dramatically decreased by CMC2.24 (5–10 μM) in a dose-dependent manner.

Suppression of the NF-κB/Hif-2α axis by CMC2.24 in SNP-stimulated chondrocytes

Immunofluorescence staining was conducted for estimating the nuclear translocation of p65 in chondrocytes in accordance with NF-κB activation by SNP. As shown in Fig. 5c, p65-positive proteins stimulated by 0.75 mM SNP accumulated in chondrocyte nuclei, and the ratio of p65 nuclear translocation was intensively suppressed by CMC2.24 treatment. Moreover, pretreatment with BMS-345541 (5 μM) greatly enhanced CMC2.24-mediated decrease in the translocation of p65 subunits to the nuclei. As shown in Fig. 6, the expression levels of MMP-3, cleaved caspase-3, RUNX2, and VEGF significantly increased, whereas Col2a1 and Bcl-2 expression levels considerably decreased in 0.75 mM SNP-stimulated group compared with those in the control group. CMC2.24 (5–10 μM) treatment can considerably reverse these trends in a dosage-dependent manner.

Whether CMC2.24 exerts a suppressive effect against the NF-κB–Hif-2α pathway in rat chondrocytes was determined by treating the cells with CMC2.24 with or without BMS-345541 (Fig. 6). Compared with pretreatment with CMC2.24 (10 μM) + SNP, pretreatment with CMC2.24 plus
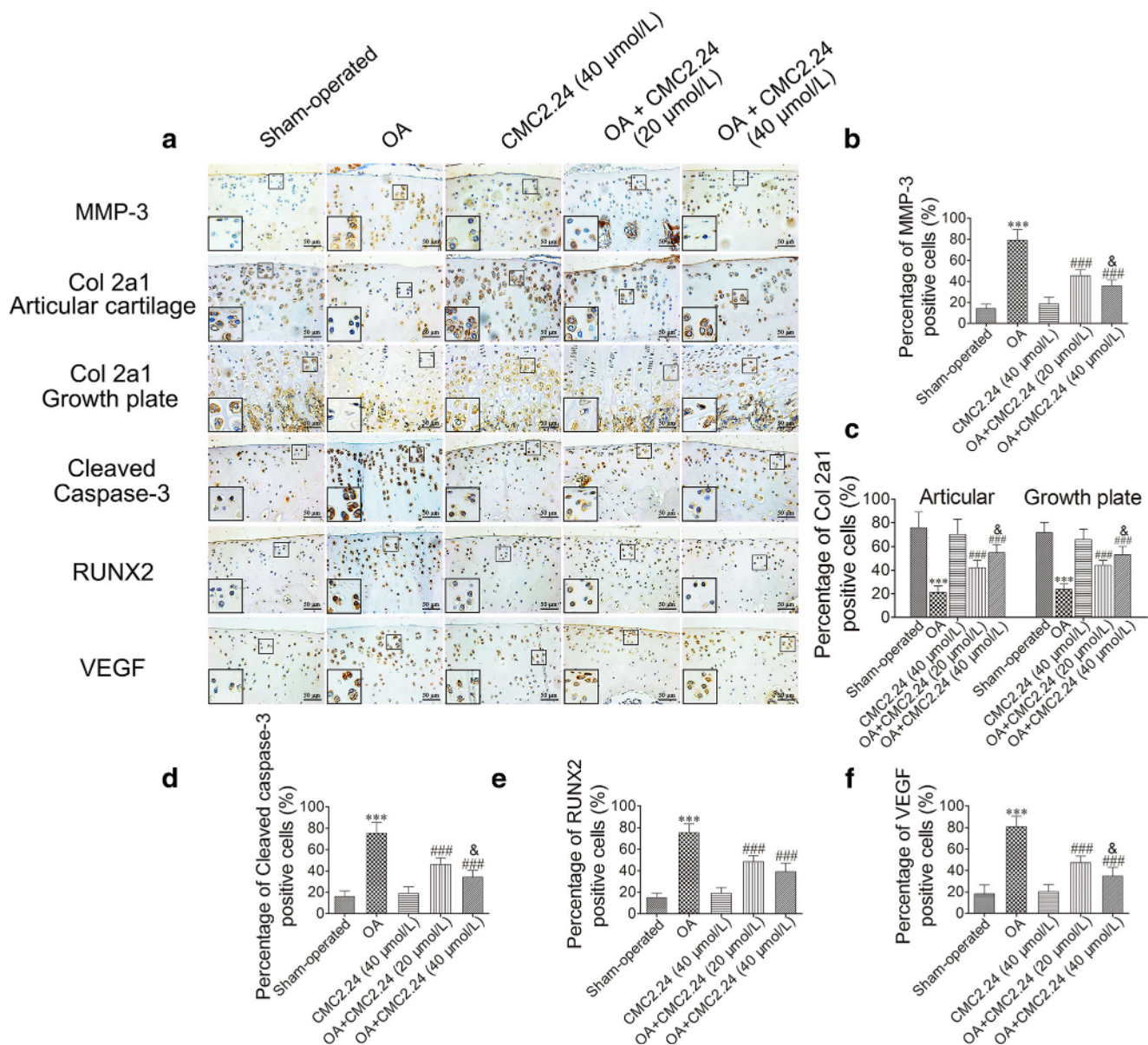
Fig. 3 Assessment of homeostasis and apoptosis in cartilage mediated by CMC2.24 in OA model rats. Sections of articular cartilage from the rats with or without CMC2.24 treatment after 10 weeks of ACLT + MMx surgery and sham operation were analyzed by immunohistochemical staining. **a** The immunohistochemical stainings of MMP-3, Col2a1, cleaved caspase-3, RUNX2, and VEGF were performed in OA model rats. The ratios of immunoreactive positive cells, MMP-3 (**b**), Col2a1 (**c**), cleaved caspase-3 (**d**), RUNX2 (**e**), and VEGF (**f**) were analyzed. Data were expressed as mean ± SEM ($n = 5$). [***]$P < 0.001$ vs. sham-operated group; [\#\#\#]$P < 0.001$ vs. OA induction group; [&]$P < 0.05$ vs. OA + CMC2.24 (20 μM) group

BMS-345541 (5 μM) decreased MMP-3, cleaved caspase-3, VEGF, and RUNX2 expression and increased Col2a1 and Bcl-2 expression. The expression of p-p65, p-IκB-α, and Hif-2α increased in the SNP-stimulated group. The administration of CMC2.24 blocked the SNP-induced up-regulation of p-p65, p-IκB-α, and Hif-2α. BMS-345541 (5 μM) remarkably enhanced CMC2.24-mediated decrease in p-p65, p-IκB-α, and Hif-2α expression. Collectively, these results indicated that CMC2.24 decreased SNP-induced chondrocyte apoptosis most likely by suppressing the NF-κB/Hif-2α axis.

On account of the evidence that CMC2.24 competitively inhibited the expression of IκB-α and NF-κB p65 in SNP-induced rat chondrocytes, we conducted docking calculation to explore the interaction between CMC2.24 and IκB/NF-κB p65 complex (Fig. 7a). The spatial filling model illustrated that CMC2.24 was fully embedded in the inhibitory pocket of IκB/NF-κB p65 homodimer complex in SNP-induced rat chondrocytes. The surface of CMC2.24 binds IκB/NF-κB p65 homodimer complex with a binding energy of − 59.00 kcal/mol.
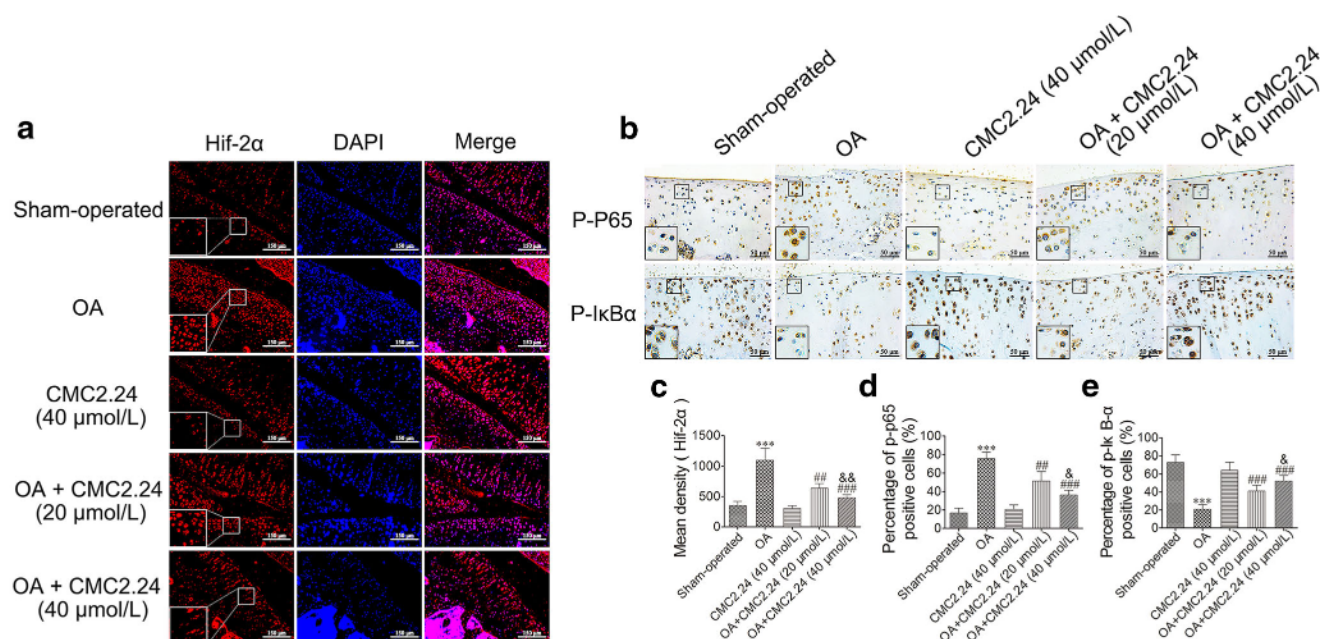
Fig. 4 Suppression of the NF-κB–Hif-2α pathway by CMC2.24 treatment in vivo in OA. **a** Immunofluorescence with an antibody to Hif-2α in articular cartilage from the rats with or without CMC2.24 treatment at 10 weeks post-surgery. The ratios of immunoreactive positive cells according to immunofluorescence. **b** Immunohistochemical staining of p-p65, p-IκB-α in ACLT + MMx-induced OA rats with the administration of PBS and CMC2.24. **c** The mean density of Hif-2α was quantified. The p-p65 (**d**) and p-IκB-α-positive (**e**) cells were quantified. Data were expressed as mean ± SEM ($n = 5$). $^{***}P < 0.001$ vs. sham-operated group; $^{\#\#}P < 0.01$ and $^{\#\#\#}P < 0.001$ vs. OA induction group; $^{\&}P < 0.05$ vs. OA + CMC2.24 (20 μM) group

Discussion

We investigated the role of CMC2.24, a triketonic chemically modified curcumin, in the modulation of ECM homeostasis and inhibition of chondrocyte apoptosis in rats and elucidated the underlying mechanisms with the NF-κB/Hif-2α axis. The results demonstrated that CMC2.24 alleviated OA progression by modulating ECM homeostasis and providing protection against chondrocyte apoptosis by suppressing the NF-κB/Hif-2α axis.

MMPs constitute a complex group of zinc-containing neutral proteolytic enzymes that play a crucial role in the degradation and turnover of ECM [31]. Inducible MMPs are activated by inflammatory mediators, nitric oxide, and reactive oxygen species, which accelerate the degradation of the articular cartilage and aggravate OA [32]. The disruption of ECM homeostasis is a key event in the pathogenesis of OA, and MMP-3, a key player in ECM homeostasis, can degrade multiple ECM components [33, 34]. MMPs are essential for the degradation and turnover of the components of the ECM, which can mediate the loss of tissue function (including cartilage and bone destruction) in various inflammations and other diseases in pathological conditions [35]. MMP-3 may indirectly promote cartilage breakdown by activating other MMPs, inducing the degradation of proteoglycans and Col2a1, the main component of cartilage ECM, and the main structural protein in joint cartilage [36]. On the base of these studies, a lead triphenolic compound, triketonic phenylaminocarbonyl CMC2.24, has been identified in vitro in cell and tissue cultures and in vivo in the various animal models of periodontitis, arthritis, diabetes, pulmonary disease, and wound healing injuries [18, 20]. Given that CMC2.24 is more soluble in aqueous media, it is an acidic triketone rather than a diketone and thus binds strongly to zinc in the catalytic domains of MMPs [25]. Therefore, CMC 2.24 is a more potent zinc-dependent MMP inhibitor than the natural compound curcumin, which is essential for inhibiting the degradation of the cartilage matrix. The in vivo results demonstrated that CMC2.24 promoted the expression of Col2a1 in growth plates and articular cartilage and inhibited the expression of MMP-3. The increased bioavailability of CMC2.24 was the key cause of weakened cartilage degeneration in rat joint cavities. Intra-articular injection was an effective method for administering CMC2.24 in OA rat knee joints. No significant difference in Mankin score between the high-dose CMC2.24 and sham-operated groups was found, indicating that high CMC2.24 concentrations did not cause joint damage. Differences in performance between the high- and low-dose groups indicated that the therapeutic efficacy of CMC2.24 is sensitive and efficient at a certain dose. Synovial inflammation plays a crucial part in the pathophysiological process of OA [37]. This result is highly convincing to CMC2.24 in local injection therapy, which can attenuate synovial inflammation in a surgically induced OA rat model.
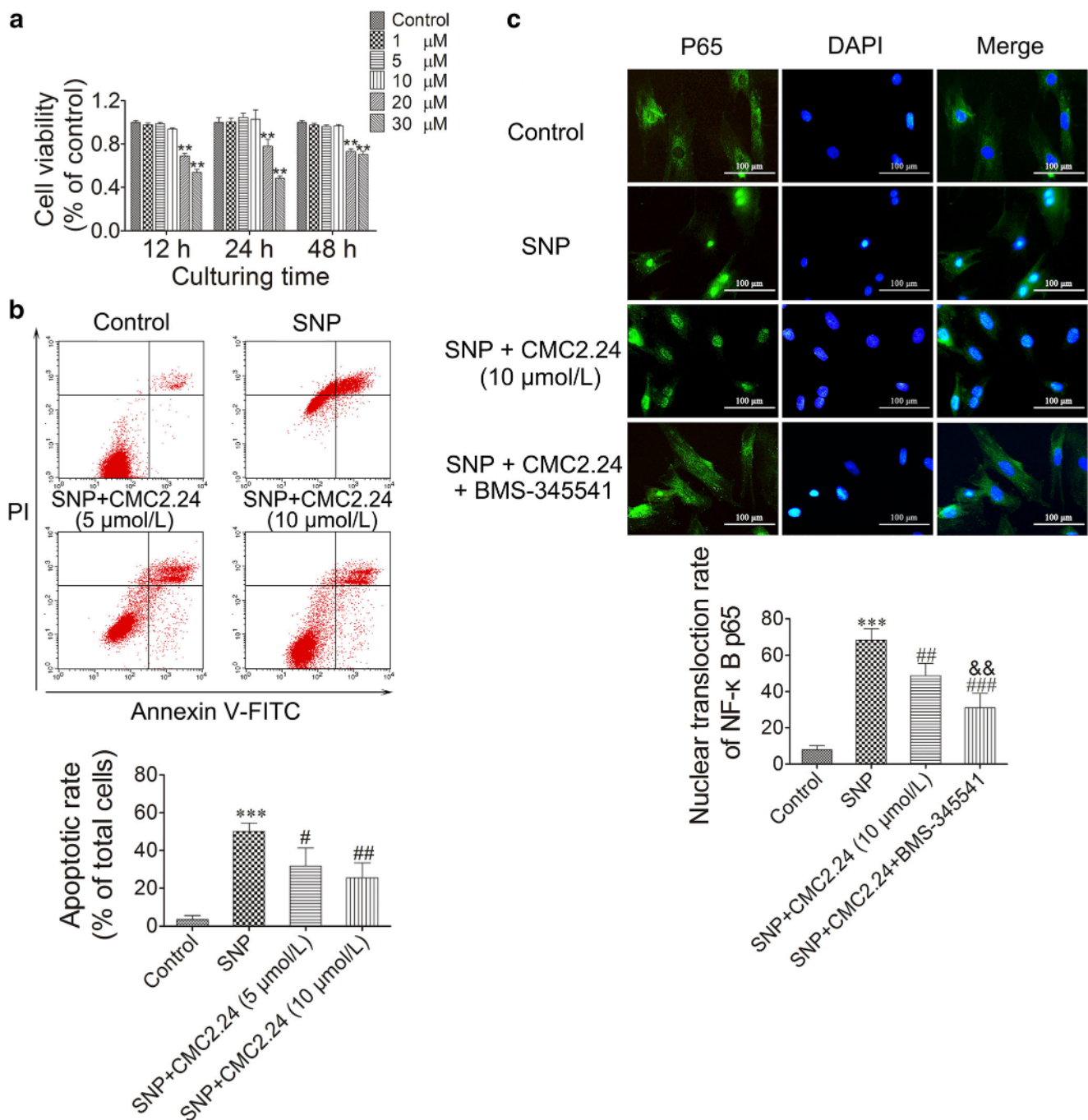
Fig. 5 CMC2.24 prevents chondrocytes from SNP-induced apoptosis and attenuates NF-κB pathway activation. **a** Cell viability were determined by CCK-8. Chondrocytes were treated with CMC2.24 at various concentrations for 12, 24 and 48 h using CCK8 assay. **b** Chondrocytes were pre-incubated with CMC2.24 (5 and 10 μM) for 2 h before 0.75 mM SNP co-treatment for 24 h. Apoptotic index was determined using FCM.

c The nuclear translocation of p65 levels was determined by immunofluorescence. Data were expressed as mean ± SEM. in CCK-8 assay ($n = 6$), FCM ($n = 3$), and immunofluorescence ($n = 3$). $^{**}P < 0.01$ and $^{***}P < 0.001$ vs. the control group; $^{#}P < 0.05$, $^{##}P < 0.01$ and $^{###}P < 0.001$ vs. the SNP group; $^{&&}P < 0.01$ vs. the SNP + CMC2.24 (10 μM) group

This involves the production of counterproductive effects and emphasizes the importance of using the lowest possible effective dose. The lowest effective dose of CMC2.24 is preferred to curcumin in the prevention of potential adverse effects. The reduction in joint synovitis observed in CMC2.24-treated animals indicated an effect on synovial fibroblast inflammatory response.

OA reflects the imbalance between catabolism and anabolism in the articular cartilage matrix, and thus, inducing anabolism or inhibiting catabolism is an effective strategy [38].
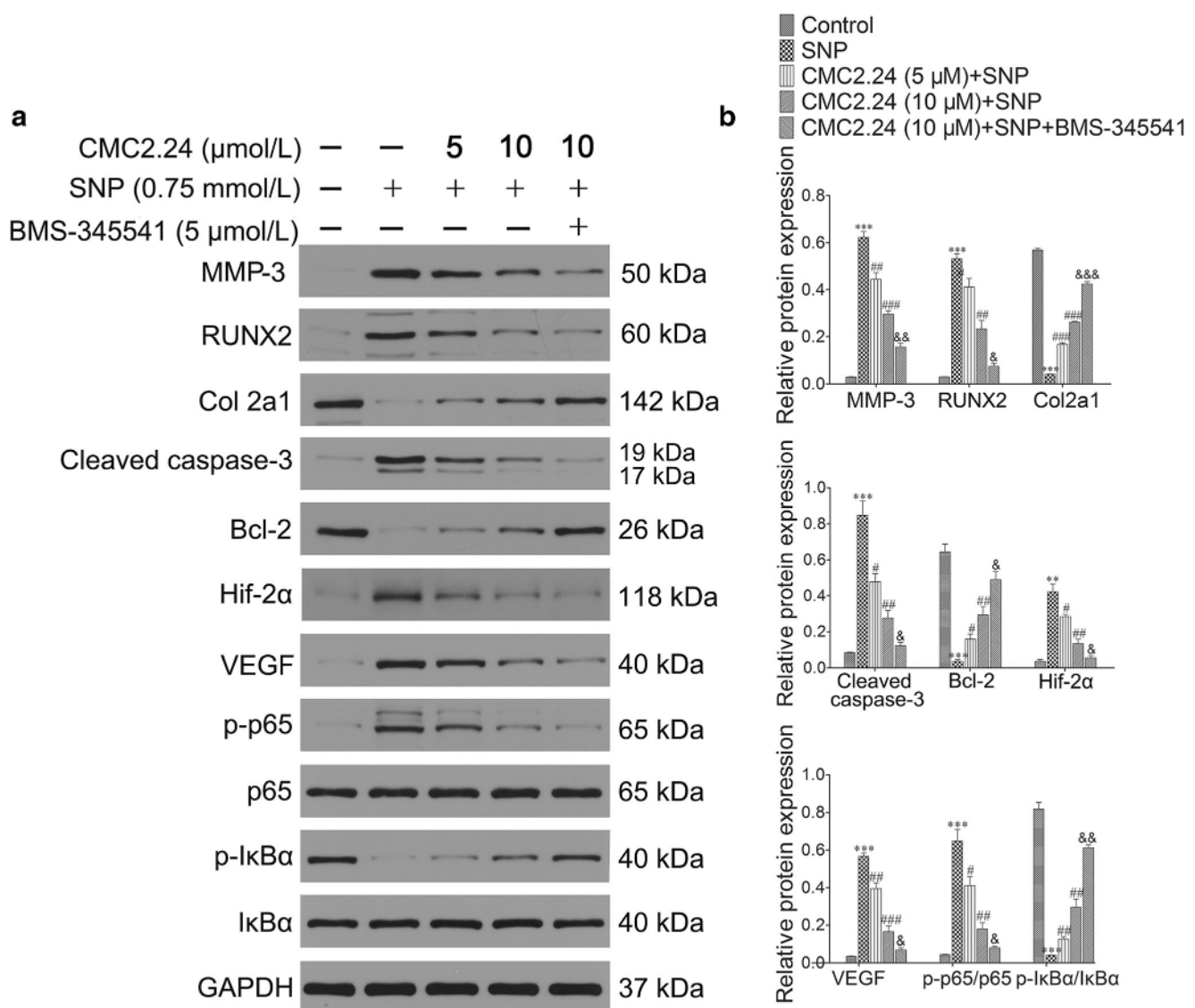
Fig. 6 Effects of CMC2.24 on the regulation of NF-κB–Hif-2α axis in SNP-induced chondrocyte catabolism and apoptosis. CMC2.24 (5 and 10 μM) was used for chondrocyte pretreatment in with or without BMS-345541 (5 μM) for 2 h prior to co-treatment using 0.75 mM SNP for 24 h. **a** The protein expression levels of MMP-3, RUNX2, Col2a1, cleaved caspase-3, Bcl-2, Hif-2α, VEGF, p-p65, p65, p-IκB-α, and IκB-α were assessed via Western blotting with GAPDH as a loading control. **b** The ratios of MMP-3, RUNX2, Col2a1, cleaved caspase-3, Bcl-2, Hif-2α, and VEGF to GAPDH were analyzed, and the ratios of p-p65/p65 and p-IκB-α/IκB-α were analyzed. Data were expressed as mean ± SEM ($n = 3$). $^{**}P < 0.01$ and $^{***}P < 0.001$ vs. the control group; $^{#}P < 0.05$, $^{##}P < 0.01$ and $^{###}P < 0.001$ vs. the SNP group; $^{&}P < 0.05$, $^{&&}P < 0.01$ and $^{&&&}P < 0.001$ vs. the SNP + CMC2.24 (10 μM) group

Hif-2α is mainly expressed in well-differentiated chondrocytes, functioning independently from oxygen-dependent hydroxylation, denying the importance of Hif-2a in the survival of cartilage under hypoxic conditions [39, 40]. In the latter or severe stages of OA, the expression of Hif2α decreases after reaching a maximum at the initiation of cartilage degradation in mice and humans, as confirmed in a previous study [41]. RUNX2 is the mediator of chondrocyte hypertrophy and MMP-3 expression in experimental mouse knee OA models after several weeks of treatment [42]. VEGF is a well-characterized growth factor that induces angiogenesis and may be the primary mediator of Hif-2α-induced osteophyte formation because it is highly expressed in the periphery of OA cartilage [43, 44]. As shown in our study, CMC 2.24 treatment in ACLT + MMx-induced OA rats prevented cartilage destruction and modulated ECM homeostasis and chondrocyte apoptosis, which was mediated by down-regulating Hif-2α expression and downstream VEGF and RUNX2 expression.

The roles of CMC2.24 in the modulation of ECM homeostasis and attenuation of apoptosis have been proposed in SNP-induced rat chondrocytes in vitro. Curcumin prevents SNP-induced apoptosis by blocking the mitochondria-dependent apoptotic pathway and maintaining the metabolic
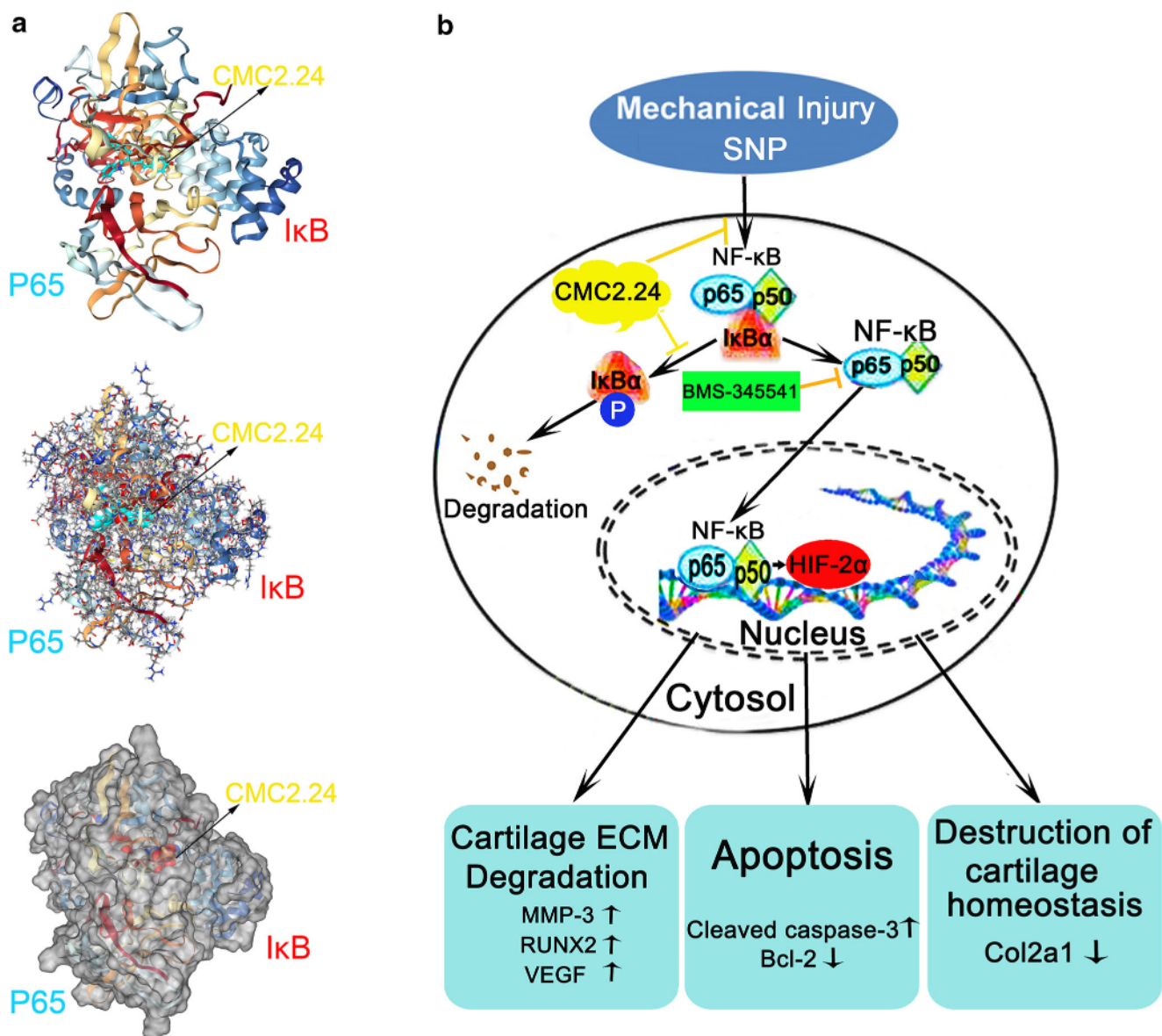
Fig. 7 The putative chondroprotective mechanism of BBR via NF-κB–Hif-2α axis. a The spatial filling model illustrated that CMC2.24 was fully embedded in the inhibitory pocket of IκB/NF-κB p65 homodimer complex in SNP-induced rat chondrocytes. The surface of CMC2.24 bind IκB/NF-κB p65 homodimer complex with the binding energies of −59.00 kcal/mol. b CMC2.24 exerts dual effects on restoring cartilage homeostasis and inhibiting chondrocyte apoptosis by inhibiting the activation of the NF-κB–Hif-2α pathway

balance in the ECM [45]. Curcumin suppresses apoptosis and inflammatory signaling through the mechanism of ERK1/2-induced chondrocyte autophagy [46]. Previous studies have shown that curcumin is involved in the modulation of apoptotic relevant signaling pathway activation and mediator production, reduction of NF-κB activation and lipid-derived inflammatory mediator production, inhibition of reactive oxygen species and reactive nitrogen species, and increase of histone deacetylase expression [47, 48]. In the present study, CMC2.24 maintained the metabolic balance of ECM at the site of cartilage degeneration and prevented cartilage tissue apoptosis by suppressing the activity of the IκB/NF-κB p65

homodimer complex. It should be noted that only total apoptotic cells but not at different stages of apoptotic cells were examined in this study, which is the limitation of the study.

Hif-2 axis signaling from NF-κB to endochondral ossification-related molecules may represent a rational therapeutic target for OA and may have minimal impact on physiological skeletal homeostasis [13, 43, 49]. In our study, SNP-induced apoptosis and matrix degradation in chondrocytes and articular cartilage were associated with the activation of the NF-κB/Hif-2α axis, leading to increases in MMP-3, RUNX2, and cleaved caspase-3 levels and decreases in Col2a1, VEGF, and Bcl-2 levels in vivo and in vitro. The

beneficial effects of CMC2.24 in OA may be due to the fact that (i) CMC2.24 optimizes many physical and chemical properties through chemical modification and improves bio-availability. (ii) CMC2.24 improves the pharmacokinetics and toxicokinetics in vivo. (iii) As a powerful inhibitor of MMP, it is highly adaptable and inhibits cartilage degeneration and ECM degradation. (iv) Intra-articular injection of CMC2.24 effectively reduces the impact of systemic toxicity and side effects upon long-term use and directly acts on the joint cavity. Basing on the present data, we propose the following working mechanism: CMC2.24 inhibits the SNP-induced phosphory-lation of IκB-α and NF-κB p65 in rat chondrocytes after reg-ulating of the NF-κB/Hif-2α axis downstream matrix anabo-lism and catabolism and chondrocyte apoptosis (Fig. 7b).

In summary, the results indicated that CMC2.24 can regu-late the activation of Col2a1 and Bcl-2 synthesis and inhibit MMP-3, RUNX2, cleaved caspase-3, and VEGF expression by modulating the NF-κB/Hif-2α axis in rat articular chondrocytes. Furthermore, CMC2.24 blocked OA develop-ment in the ACLT + MMx-induced OA rat model. This result indicates that CMC2.24 is a new therapeutic agent in OA.

Compliance with ethical standards

Conflict of interest The authors declare that they have no conflict of interest.

Ethical approval This study was approved by the Animal Care and Use Committee of Medical School, Wuhan University. All of the protocols were approved by the Institutional Ethics Committee of Medical School, Wuhan University.

References

1. Choi WS, Yang JI, Kim W, Kim HE, Kim SK, Won Y, Son YO, Chun CH, Chun JS (2019) Critical role for arginase II in osteoar-thritis pathogenesis. Ann Rheum Dis 78:421–428
2. Guilak F, Nims RJ, Dicks A, Wu CL, Meulenbelt I (2018) Osteoarthritis as a disease of the cartilage pericellular matrix. Matrix Biol 71-72:40–50
3. Kraus VB, Simon LS, Katz JN, Neogi T, Hunter D, Guermazi A, Karsdal MA (2019) Proposed study designs for approval based on a surrogate endpoint and a post-marketing confirmatory study under FDA's accelerated approval regulations for disease modifying oste-oarthritis drugs. Osteoarthr Cartil 27:571–579
4. Geyer M, Schonfeld C (2018) Novel insights into the pathogenesis of osteoarthritis. Curr Rheumatol Rev 14:98–107
5. Hu G, Zhao X, Wang C, Geng Y, Zhao J, Xu J, Zuo B, Zhao C, Wang C, Zhang X (2017) MicroRNA-145 attenuates TNF-alpha-driven cartilage matrix degradation in osteoarthritis via direct sup-pression of MKK4. Cell Death Dis 8:e3140
6. Yang CY, Chanalaris A, Troeberg L (2017) ADAMTS and ADAM metalloproteinases in osteoarthritis - looking beyond the 'usual sus-pects'. Osteoarthr Cartil 25:1000–1009
7. Hunter DJ, Bierma-Zeinstra S (2019) Osteoarthritis. Lancet 393: 1745–1759
8. Hwang HS, Kim HA (2015) Chondrocyte apoptosis in the patho-genesis of osteoarthritis. Int J Mol Sci 16:26035–26054
9. Musumeci G, Castrogiovanni P, Trovato FM, Weinberg AM, Al-Wasiyah MK, Alqahtani MH, Mobasheri A (2015) Biomarkers of chondrocyte apoptosis and autophagy in osteoarthritis. Int J Mol Sci 16:20560–20575
10. Hirata M, Kugimiya F, Fukai A, Saito T, Yano F, Ikeda T, Mabuchi A, Sapkota BR, Akune T, Nishida N, Yoshimura N, Nakagawa T, Tokunaga K, Nakamura K, Chung UI, Kawaguchi H (2012) C/EBPbeta and RUNX2 cooperate to degrade cartilage with MMP-13 as the target and HIF-2alpha as the inducer in chondrocytes. Hum Mol Genet 21:1111–1123
11. Inoue H, Arai Y, Kishida T, Terauchi R, Honjo K, Nakagawa S, Tsuchida S, Matsuki T, Ueshima K, Fujiwara H, Mazda O, Kubo T (2015) Hydrostatic pressure influences HIF-2 alpha expression in chondrocytes. Int J Mol Sci 16:1043–1050
12. Murahashi Y, Yano F, Kobayashi H, Makii Y, Iba K, Yamashita T, Tanaka S, Saito T (2018) Intra-articular administration of IkappaBalpha kinase inhibitor suppresses mouse knee osteoarthritis via downregulation of the NF-kappaB/HIF-2alpha axis. Sci Rep 8: 16475
13. Choi MC, Choi WH (2018) Mithramycin a alleviates osteoarthritic cartilage destruction by inhibiting HIF-2alpha expression. Int J Mol Sci 19:1411
14. Lepetsos P, Papavassiliou KA, Papavassiliou AG (2019) Redox and NF-kappaB signaling in osteoarthritis. Free Radic Biol Med 132:90–100
15. Kobayashi H, Chang SH, Mori D, Itoh S, Hirata M, Hosaka Y, Taniguchi Y, Okada K, Mori Y, Yano F, Chung UI, Akiyama H, Kawaguchi H, Tanaka S, Saito T (2016) Biphasic regulation of chondrocytes by Rela through induction of anti-apoptotic and cat-abolic target genes. Nat Commun 7:13336
16. Oh H, Kwak JS, Yang S, Gong MK, Kim JH, Rhee J, Kim SK, Kim HE, Ryu JH, Chun JS (2015) Reciprocal regulation by hypoxia-inducible factor-2alpha and the NAMPT-NAD(+)-SIRT axis in ar-ticular chondrocytes is involved in osteoarthritis. Osteoarthr Cartil 23:2288–2296
17. Saito T, Fukai A, Mabuchi A, Ikeda T, Yano F, Ohba S, Nishida N, Akune T, Yoshimura N, Nakagawa T, Nakamura K, Tokunaga K, Chung UI, Kawaguchi H (2010) Transcriptional regulation of en-dochondral ossification by HIF-2alpha during skeletal growth and osteoarthritis development. Nat Med 16:678–686
18. Golub LM, Lee HM (2020) Periodontal therapeutics: current host-modulation agents and future directions. Periodontol 82:186–204
19. Deng J, Golub LM, Lee HM, Lin MC, Bhatt HD, Hong HL, Johnson F, Scaduto J, Zimmerman T, Gu Y (2020) Chemically-modified curcumin 2.24: a novel systemic therapy for natural peri-odontitis in dogs. J Exp Pharmacol 12:47–60
20. Wang HH, Lee HM, Raja V, Hou W, Iacono VJ, Scaduto J, Johnson F, Golub LM, Gu Y (2019) Enhanced efficacy of chemi-cally modified curcumin in experimental periodontitis: systemic implications. J Exp Pharmacol 11:1–14
21. Mirzaei H, Shakeri A, Rashidi B, Jalili A, Banikazemi Z, Sahebkar A (2017) Phytosomal curcumin: a review of pharmacokinetic, ex-perimental and clinical studies. Biomed Pharmacother 85:102–112

22. Arshad L, Haque MA, Abbas Bukhari SN, Jantan I (2017) An overview of structure-activity relationship studies of curcumin analogs as antioxidant and anti-inflammatory agents. Future Med Chem 9:605–626

23. Moon DO, Kim MO, Choi YH, Park YM, Kim GY (2010) Curcumin attenuates inflammatory response in IL-1beta-induced human synovial fibroblasts and collagen-induced arthritis in mouse model. Int Immunopharmacol 10:605–610

24. Xu Y, Ge L, Abdel-Razek O, Jain S, Liu Z, Hong Y, Nieman G, Johnson F, Golub LM, Cooney RN, Wang G (2016) Differential susceptibility of human SP-b genetic variants on lung injury caused by bacterial pneumonia and the effect of a chemically modified CURCUMIN. Shock 45:375–384

25. Zhang Y, Gu Y, Lee HM, Hambardjieva E, Vrankova K, Golub LM, Johnson F (2012) Design, synthesis and biological activity of new polyenolic inhibitors of matrix metalloproteinases: a focus on chemically-modified curcumins. Curr Med Chem 19:4348–4358

26. Zhang Y, Golub LM, Johnson F, Wishnia A (2012) pKa, zinc- and serum albumin-binding of curcumin and two novel biologically-active chemically-modified curcumins. Curr Med Chem 19:4367–4375

27. Antonelli AC, Zhang Y, Golub LM, Johnson F, Simon SR (2014) Inhibition of anthrax lethal factor by curcumin and chemically modified curcumin derivatives. J Enzyme Inhib Med Chem 29:663–669

28. Coury JR, Nixon R, Collins M, Schwartz J, Chahine NO, Grande DA (2018) Oral administration of a chemically modified curcumin, TRB-N0224, reduced inflammatory cytokines and cartilage erosion in a rabbit ACL transection injury model. Cartilage: 1947603518815263. https://doi.org/10.1177/1947603518815263

29. Zhou Y, Liu SQ, Yu L, He B, Wu SH, Zhao Q, Xia SQ, Mei HJ (2015) Berberine prevents nitric oxide-induced rat chondrocyte apoptosis and cartilage degeneration in a rat osteoarthritis model via AMPK and p38 MAPK signaling. Apoptosis 20:1187–1199

30. Hayami T, Pickarski M, Zhuo Y, Wesolowski GA, Rodan GA, Duong LT (2006) Characterization of articular cartilage and subchondral bone changes in the rat anterior cruciate ligament transection and meniscectomized models of osteoarthritis. Bone 38: 234–243

31. Son YO, Park S, Kwak JS, Won Y, Choi WS, Rhee J, Chun CH, Ryu JH, Kim DK, Choi HS, Chun JS (2017) Estrogen-related receptor gamma causes osteoarthritis by upregulating extracellular matrix-degrading enzymes. Nat Commun 8:2133

32. Alshenibr W, Tashkandi MM, Alsaqer SF, Alkheriji Y, Wise A, Fulzele S, Mehra P, Goldring MB, Gerstenfeld LC, Bais MV (2017) Anabolic role of lysyl oxidase like-2 in cartilage of knee and temporomandibular joints with osteoarthritis. Arthritis Res Ther 19:179

33. Jeon J, Kang LJ, Lee KM, Cho C, Song EK, Kim W, Park TJ, Yang S (2018) 3'-Sialyllactose protects against osteoarthritic development by facilitating cartilage homeostasis. J Cell Mol Med 22:57–66

34. Zhou S, Lu W, Chen L, Ge Q, Chen D, Xu Z, Shi D, Dai J, Li J, Ju H, Cao Y, Qin J, Chen S, Teng H, Jiang Q (2017) AMPK deficiency in chondrocytes accelerated the progression of instability-induced and ageing-associated osteoarthritis in adult mice. Sci Rep 7:43245

35. Tu C, Ma Y, Song M, Yan J, Xiao Y, Wu H (2019) Liquiritigenin inhibits IL-1beta-induced inflammation and cartilage matrix degradation in rat chondrocytes. Eur J Pharmacol 858:172445

36. Cheleschi S, Fioravanti A, De Palma A, Corallo C, Franci D, Volpi N, Bedogni G, Giannotti S, Giordano N (2018) Methylsulfonylmethane and mobilee prevent negative effect of IL-1beta in human chondrocyte cultures via NF-kappaB signaling pathway. Int Immunopharmacol 65:129–139

37. Ashraf S, Mapp PI, Shahtaheri SM, Walsh DA (2018) Effects of carrageenan induced synovitis on joint damage and pain in a rat model of knee osteoarthritis. Osteoarthr Cartil 26:1369–1378

38. Singh P, Marcu KB, Goldring MB, Otero M (2019) Phenotypic instability of chondrocytes in osteoarthritis: on a path to hypertrophy. Ann N Y Acad Sci 1442:17–34

39. Yang S, Ryu JH, Oh H, Jeon J, Kwak JS, Kim JH, Kim HA, Chun CH, Chun JS (2015) NAMPT (visfatin), a direct target of hypoxia-inducible factor-2alpha, is an essential catabolic regulator of osteoarthritis. Ann Rheum Dis 74:595–602

40. Zhang FJ, Luo W, Lei GH (2015) Role of HIF-1alpha and HIF-2alpha in osteoarthritis. Joint Bone Spine 82:144–147

41. Thoms BL, Dudek KA, Lafont JE, Murphy CL (2013) Hypoxia promotes the production and inhibits the destruction of human articular cartilage. Arthritis Rheum 65:1302–1312

42. Saito T, Nishida K, Furumatsu T, Yoshida A, Ozawa M, Ozaki T (2013) Histone deacetylase inhibitors suppress mechanical stress-induced expression of RUNX-2 and ADAMTS-5 through the inhibition of the MAPK signaling pathway in cultured human chondrocytes. Osteoarthr Cartil 21:165–174

43. Saito T, Kawaguchi H (2010) HIF-2alpha as a possible therapeutic target of osteoarthritis. Osteoarthr Cartil 18:1552–1556

44. Ishizuka S, Sakai T, Hiraiwa H, Hamada T, Knudson W, Omachi T, Ono Y, Nakashima M, Matsukawa T, Oda T, Takamatsu A, Yamashita S, Ishiguro N (2016) Hypoxia-inducible factor-2alpha induces expression of type X collagen and matrix metalloproteinases 13 in osteoarthritic meniscal cells. Inflamm Res 65:439–448

45. Zhao P, Cheng J, Geng J, Yang M, Zhang Y, Zhang Q, Wang Y, Lu B (2018) Curcumin protects rabbit articular chondrocytes against sodium nitroprusside-induced apoptosis in vitro. Eur J Pharmacol 828:146–153

46. Li X, Feng K, Li J, Yu D, Fan Q, Tang T, Yao X, Wang X (2017) Curcumin inhibits apoptosis of chondrocytes through activation ERK1/2 signaling pathways induced autophagy. Nutrients 9:414

47. Chin KY (2016) The spice for joint inflammation: anti-inflammatory role of curcumin in treating osteoarthritis. Drug Des Devel Ther 10:3029–3042

48. Henrotin Y, Clutterbuck AL, Allaway D, Lodwig EM, Harris P, Mathy-Hartert M, Shakibaei M, Mobasheri A (2010) Biological actions of curcumin on articular chondrocytes. Osteoarthr Cartil 18:141–149

49. Pi Y, Zhang X, Shao Z, Zhao F, Hu X, Ao Y (2015) Intra-articular delivery of anti-Hif-2alpha siRNA by chondrocyte-homing nanoparticles to prevent cartilage degeneration in arthritic mice. Gene Ther 22:439–448